

March 19, 2014

MoS₂ functionalization for ultra-thin atomic layer deposited dielectrics

Angelica Azcatl, *University of Texas at Dallas*

Stephen McDonnell, *University of Texas at Dallas*

Santosh KC, *University of Texas at Dallas*

Xin Peng, *University of Texas at Dallas*

Hong Dong, *University of Texas at Dallas*, et al.

MoS₂ functionalization for ultra-thin atomic layer deposited dielectrics

Angelica Azcatl,¹ Stephen McDonnell,¹ Santosh K. C.,¹ Xin Peng,¹ Hong Dong,¹ Xiaoye Qin,¹ Rafik Addou,¹ Greg I. Mordj,² Ning Lu,¹ Jiyoung Kim,^{1,2} Moon J. Kim,¹ Kyeongjae Cho,¹ and Robert M. Wallace^{1,a)}

¹Department of Materials Science and Engineering, The University of Texas at Dallas, 800 West Campbell Road, Richardson, Texas 75080, USA

²Department of Electrical Engineering, The University of Texas at Dallas, 800 West Campbell Road, Richardson, Texas 75080, USA

(Received 28 December 2013; accepted 9 March 2014; published online 19 March 2014)

The effect of room temperature ultraviolet-ozone (UV-O₃) exposure of MoS₂ on the uniformity of subsequent atomic layer deposition of Al₂O₃ is investigated. It is found that a UV-O₃ pre-treatment removes adsorbed carbon contamination from the MoS₂ surface and also functionalizes the MoS₂ surface through the formation of a weak sulfur-oxygen bond without any evidence of molybdenum-sulfur bond disruption. This is supported by first principles density functional theory calculations which show that oxygen bonded to a surface sulfur atom while the sulfur is simultaneously back-bonded to three molybdenum atoms is a thermodynamically favorable configuration. The adsorbed oxygen increases the reactivity of MoS₂ surface and provides nucleation sites for atomic layer deposition of Al₂O₃. The enhanced nucleation is found to be dependent on the thin film deposition temperature. © 2014 AIP Publishing LLC. [<http://dx.doi.org/10.1063/1.4869149>]

As scaling of the silicon-based complementary metal-oxide-semiconductor is reaching its physical limits,¹ two dimensional (2-D) transition metal dichalcogenides (TMDs) are being considered as ideal candidates for channel materials in field effect transistors (FETs) due to their atomic thickness and bandgap comparable to that of silicon.² Recent efforts in the integration of 2-D materials such as MoS₂ have reported promising electron mobilities, on/off ratios of $\sim 10^8$, and low interface trap densities, D_{it} .³⁻⁹ Yet, uniform deposition of sub-10 nm dielectrics on 2-D materials remains challenging. For example, when ~ 15 – 17 nm HfO₂ is deposited by atomic layer deposition (ALD) on clean MoS₂, island type growth is observed resulting in non-uniform films.¹⁰ In the case of Al₂O₃ ALD, uniform films of ~ 10 nm in thickness have been reported.¹¹ In contrast, when performing ALD using the same temperature, precursors, and thickness, non-uniform ALD of Al₂O₃ has been reported.¹² The use of solvent-based pre-cleaning steps of the MoS₂ surface may explain the contradiction between such results.¹⁰

The examples of non-uniform ALD on MoS₂ emphasize that surface pre-treatments (or chemical residues) are needed in order to promote reactivity with the ALD precursors, similar to graphene.^{13,15} Different surface treatments to improve nucleation of dielectric films deposited by ALD on graphene have been utilized,¹⁶ which include functionalization with nitrogen dioxide NO₂, remotely generated O₃, and metal oxide deposition.¹⁷⁻¹⁹ An oxygen plasma treatment has recently been demonstrated to improve coverage of ALD-Al₂O₃ (or HfO₂) on multilayer MoS₂ flakes.¹² Though dielectric films were obtained by this method, the improved nucleation was shown to be due to the oxidation of MoS₂. The MoO₃ formed during the plasma treatment would likely

affect the electrical properties at the MoS₂ surface due to bond disruption and/or band alignments (i.e., MoO₃ is a semiconductor with a wide band gap of ~ 3.1 eV,²⁰ whereas the monolayer MoS₂ band gap is 1.8 eV (Ref. 21)). Consequently, the use of such plasma treatments may degrade interface quality in multi-layer MoS₂ devices and would be impractical for monolayer-based devices.

In this Letter, a non-destructive method is proposed to functionalize MoS₂ by ultraviolet (UV)-O₃ exposure, where formation of oxygen-sulfur bonds at the top sulfur layer on the surface was achieved without breaking sulfur-molybdenum bonds (i.e., no formation of MoO₃). Additionally, first principles calculations show that the thermodynamics of the O₃ interaction with MoS₂ subsequently produces stable bonding upon oxygen absorption on MoS₂. It is demonstrated that the oxygen functionalized MoS₂ surface (“O-SMoS”) is an ideal nucleation layer for ALD, allowing deposition of fully-covered and uniform Al₂O₃ thin films of ~ 4 nm on MoS₂. This result highlights the importance of the UV-O₃ treatment as a route toward high quality ultra-thin dielectrics on TMDs.

An *in situ* study of UV-O₃ exposure of MoS₂ was performed to monitor chemical state changes by monochromatic Al K α X-ray Photoelectron Spectroscopy (XPS), without exposure of samples to the environment to avoid spurious contamination. Details of the instrument were described previously²² and in the supplementary material.²³ A bulk MoS₂ crystal (SPI Supplies) was mechanically exfoliated using Scotch[®] Magic[™] Tape to remove the top most layers. The sample was loaded into ultrahigh vacuum (UHV) within 5 min and transferred to a chamber to perform the UV-O₃ treatment. Ozone was produced by UV photons from a low pressure mercury lamp^{22,24,25} at an O₂ pressure of P_{O₂} = 900 millibar within a few mm of the sample surface. The ALD experiments were performed in an attached Picoson

^{a)}Electronic mail: rmwallace@utdallas.edu

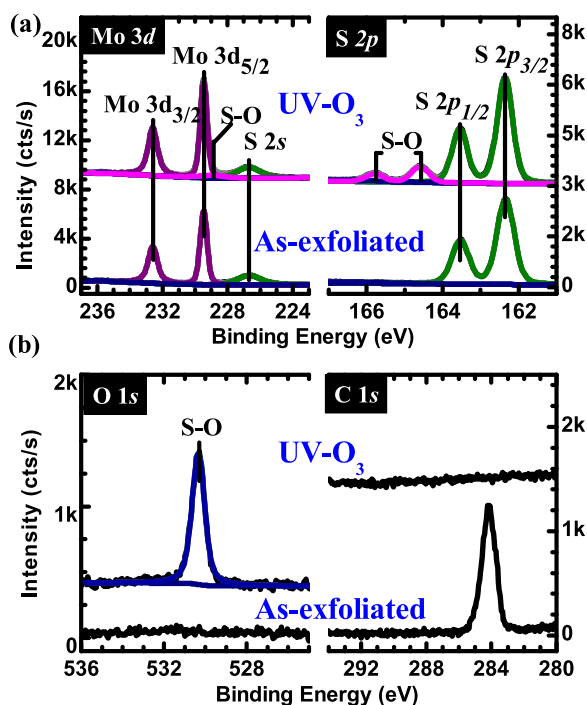


FIG. 1. X-ray photoelectron spectra corresponding to the (a) $S2p$, $Mo\ 3d$ and (b) $O\ 1s$, $C\ 1s$ core levels of the initial as-exfoliated bulk MoS_2 and after $UV-O_3$ treatment. $k = 1000$.

SUNALETM ALD reactor ($P_{base} \cong 0.1$ millibar) allowing for deposition and analysis without air exposure. Trimethylaluminum (TMA) and H_2O were used as the metal and oxidant precursors, respectively. The precursor pulse and purge times were 0.1 and 4 s, respectively, at $P \cong 10$ mbar, using ultra-high purity N_2 as the carrier and purging gas.

XPS of the initial, as-exfoliated MoS_2 surface are shown in Figure 1. The oxygen concentration is confirmed to be below the limit of detection while C (~ 0.5 monolayer (ML)), in a mixture of graphitic and sp^3 hydrocarbons, is the only detectable contaminant on the *ex situ* exfoliated MoS_2 and likely to originate from the environment after the exfoliation process.

After $UV-O_3$ exposure, the $S\ 2p$ spectrum shows an additional doublet peak at 164.8 eV (Fig. 1(a)), which is concurrent with the appearance of an $O\ 1s$ peak (Fig. 1(b)), and suggests oxidation of sulfur. The increase in the binding energy position of this $S\ 2p$ feature indicates that sulfur is no longer in the S^{2-} oxidation state of MoS_2 , yet lower than that of S^{4+} previously reported after MoS_2 oxidation by a RF-oxygen plasma.²⁴ Considering the $Mo\ 3d$ states, (see Fig. 1(a), *viz.* no detectable Mo-Mo or Mo-O formation), the change in the sulfur oxidation state is likely due to the formation of covalent S-O bonding without Mo-S bond

scission. Note that the S-O feature observed in the $S\ 2p$ core-level must also be present in the $S\ 2s$. The spectral deconvolution of the $Mo\ 3d$ and $S\ 2s$ core-level is achieved with an S-O feature in the $S\ 2s$ with an identical core-level chemical shift and appropriate intensity relative to the $S\ 2p$. Using the peak intensity ratio I_{S-O}/I_S (see supplementary material),²³ the oxygen coverage on MoS_2 was calculated to be ~ 1 monolayer, which suggests that only the MoS_2 surface is oxygen functionalized. It was also found that the S:O ratio from the newly formed S-O bond was $\sim 1:1.3$, indicating that oxygen could be not only bonded on top of each surface sulfur atom but also could occupy interstitial sites or sulfur vacancies. Analysis of several samples indicated that the S:Mo ratio remained constant after $UV-O_3$ treatment. Additionally, as shown in Figure 1(b), the $C\ 1s$ feature is not detectable after $UV-O_3$ treatment, likely through CO and/or CO_2 formation, consistent with other semiconductor surfaces,^{25–27} without causing photochemical degradation as can occur for graphene.^{28,29}

The effect of O_3 exposure from a remote generator source on MoS_2 without UV illumination was also investigated (see supplementary material)²³ using similar pressure and temperature conditions as that used for $UV-O_3$ treatments. However, S-O bonding or Mo-oxidation were below detectable limits. Thus, UV illumination appears to be essential for the S-O bond formation under the conditions employed here. It has been shown that UV light can increase the reactivity of O_3 by up to four orders of magnitude,³⁰ and the radical O^* generated by O_2 dissociation by UV-absorption^{24,25} are expected to accelerate the oxidation process. Moreover, MoS_2 is known to be a resistant material against photodegradation, because optical transitions occur between the *d*-states.³¹ Only nanoscale MoS_2 clusters have been reported to be photochemically active for $\lambda > 400$ nm.³² Since the reactivity of MoS_2 is negligible upon UV-light irradiation, the MoS_2 surface is not likely to catalyze or be involved in the O_3 or O_2 dissociation. Further studies of ozone functionalization of MoS_2 without UV illumination will be presented elsewhere.

The density functional theory (DFT) modeling (Fig. 2(a)) indicates that an oxygen adatom has two possible adsorption sites: Oxygen atop sulfur (O_{ads}) and substitutional oxygen on a sulfur vacancy (O_S), having formation energies of -0.81 eV and -1.88 eV, respectively. A study of the exfoliated MoS_2 surface defects shows that defects (likely clusters of sulfur vacancies) cover only 0.1%–5% of the surface.³³ Thus, the ~ 1 ML coverage of S-O species observed here suggests that the O_S sites would have concentrations below the limit of detection of XPS. Importantly, the DFT result highlights that the formation of S-O bonds is energetically favorable and can occur without Mo-S scission,

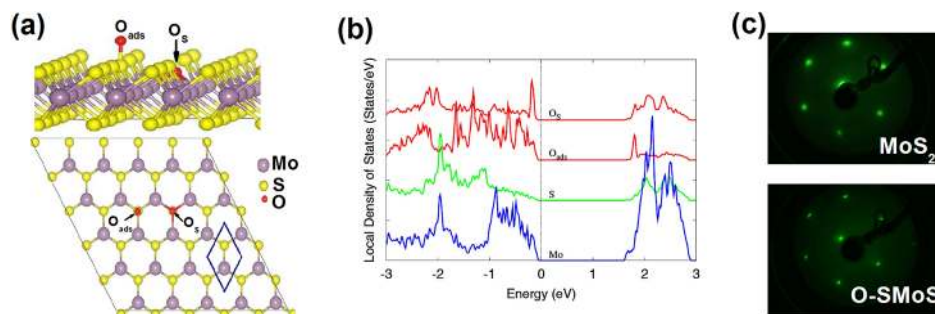


FIG. 2. (a) (5×5) supercell of MoS_2 showing the most energetically stable adsorption sites for oxygen: Oxygen on top of sulfur (O_{ads}) and substitutional oxygen on a sulfur vacancy (O_S). (b) DOS of MoS_2 generated upon O chemisorption on O_{ads} and O_S adsorption sites. (c) LEED pattern of the initial as-exfoliated MoS_2 surface (top) and after $UV-O_3$ treatment (bottom) taken at a beam energy of 127 eV.

consistent with the Mo and S chemical states observed. Moreover, the density of states (DOS) calculation shows that for low coverages of O adatoms (~ 0.1 ML), no gap states exist in the band gap, but rather shallow states at the band edge are created (Fig. 2(b)).

The calculation also shows that S mono-vacancy formation energy is relatively large (~ 2.45 eV) and a S di-vacancy is less favorable than mono-vacancy, consistent with a recent report,³² and that O is unlikely to replace S. However, mechanically exfoliated MoS₂ can create S vacancies compared to formation under thermodynamic equilibrium. The first principle calculations are therefore consistent with the detection of O-S bond formation without detectable O-Mo formation, as the sulfur vacancy concentration is not likely to be increased by UV-O₃ exposure.

The low energy electron diffraction (LEED) pattern (Fig. 2(c)) compares the as-exfoliated MoS₂ surface before and after UV-O₃ treatment. The characteristic hexagonal pattern of the unreconstructed MoS₂ (0001) surface^{34,35} was obtained for the as-exfoliated surface, with the diffraction spot spacing remaining constant after the oxygen chemisorption. Sharper spots observed after UV-O₃ treatment are likely due to the reaction and desorption of the surface carbon contamination.^{14,22,24,25} The fact that the hexagonal pattern spacing is not altered, suggests that the oxygen adsorption sites are well-defined and is in agreement with the most probable adsorption sites for oxygen, O_{ads} and O_S, calculated by DFT.

The use of Al₂O₃ as a dielectric material has been extended to 2-D materials based-devices, where the film thicknesses ranged from 10 to 50 nm.^{6,7,36} As noted earlier, nucleation of dielectrics on 2-D materials is limited by the dearth of dangling bonds on these surfaces. However, for nanoelectronic applications, pin-hole free thin film high-k dielectrics with a uniform thickness are required. To explore growth and uniformity, ALD of Al₂O₃ on O-SMoS was investigated. Atomic force microscopy (AFM) images (Fig. 3(a)) show Al₂O₃ deposited on the as-exfoliated MoS₂ at 200 °C, 250 °C, and 300 °C (typical for ALD processing³²) using 30 cycles of TMA/H₂O. It is evident that the nucleation occurs sporadically, being favored at step edges. The density of clusters on the surface is higher at lower

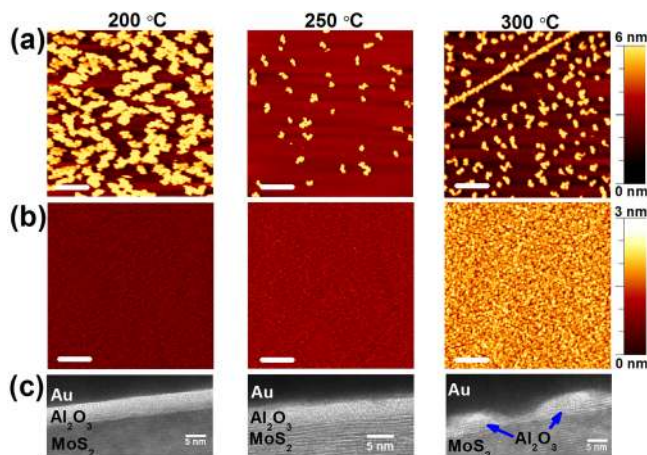


FIG. 3. Atomic force microscopy images of Al₂O₃ deposited by 30 ALD cycles at 200 °C, 250 °C, and 300 °C on (a) as exfoliated bulk MoS₂ and (b) oxygen functionalized MoS₂ (O-SMoS). Scale bar: 200 nm (c) HRTEM images of the corresponding films shown in (b).

temperatures, which is in agreement with prior reports.¹² This also demonstrates that the previous report of uniform Al₂O₃ after 110 cycles¹¹ is likely caused by functionalization due to organic contaminants on the MoS₂ surface.¹⁰

In contrast, Al₂O₃ ALD on O-SMoS results in a significant increase in coverage (Fig. 3(b)). The Al₂O₃ films showed root-mean-squared (RMS) roughness values of only 0.14 nm, 0.17 nm, and 0.30 nm, for deposition temperatures of 200 °C, 250 °C, and 300 °C, respectively.

The corresponding high-resolution transmission electron microscopy (HRTEM) cross-section images of Al₂O₃ on O-SMoS are shown in Figure 3(c). The amorphous nature of the Al₂O₃ and the characteristic layered structure of MoS₂, which is preserved after the UV-O₃ treatment, is evident as is a sharp interface between both materials. Fully-covered Al₂O₃ films were obtained at 200 °C, with a thickness of ~ 4 nm, which remains constant for the analyzed area (see supplementary material). Similar films were obtained at 250 °C, with the primary difference being an increase in surface roughness. However, films deposited at 300 °C exhibit island-type growth, which is consistent with the appearance of pin-holes of ~ 1 nm in extent for the corresponding AFM image for that temperature (Fig. 3(b)). Thus, it can be concluded that a dependence of film uniformity with deposition temperature exists.

The RMS roughness increase with deposition temperature suggests that the oxygen functionalization layer might not be stable at temperatures greater than 200 °C. To test this hypothesis, identical O-SMoS samples were prepared and then exposed to the same deposition temperatures in the ALD reactor for 20 min under N₂, at ~ 10 mbar without precursor exposure. It was found that the S-O peak intensity decreased to 30%, 10%, and 0% of the initial O-SMoS at temperatures of 200 °C, 250 °C, and 300 °C, respectively, while the S/Mo ratio remains constant after annealing (see supplementary material). Therefore, it is found that partial or total desorption of the chemisorbed oxygen occurred at these temperatures. This limited thermal stability of the S-O bond explains the results shown in Figure 3, since desorption of oxygen corresponds to depletion of nucleation sites for subsequent ALD growth, resulting in less uniform films with increasing deposition temperature.

The corresponding XPS spectra are shown in Figure 4. After Al₂O₃ deposition, the S-O bonds are no longer detected

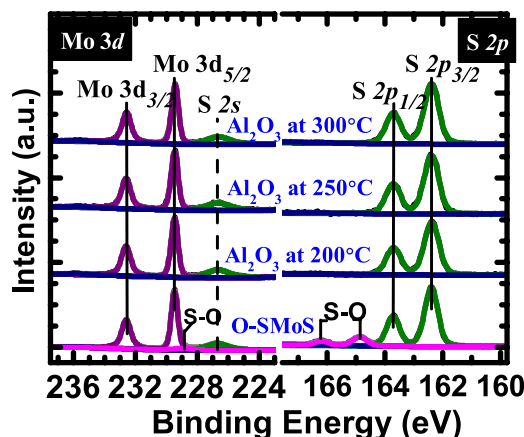


FIG. 4. XPS spectra of the S 2p and Mo 3d core level of Al₂O₃ on oxygen functionalized MoS₂ (O-SMoS) films shown in Figure 3(b).

in the S $2p$ core-level spectrum, and the chemical states of Mo and S are the same as the initial MoS₂. This was observed for all temperatures investigated, and two possible mechanisms are considered which may contribute to S-O bond scission. First, the thermal desorption of oxygen is more likely to occur when temperature is increased. Since the total deposition time for the 30 cycle films considered in this study is ~ 10 min and detectable S-O bonds are observed after 20 min annealing to 200 and 250 °C, thermal desorption alone cannot explain the complete removal of the S-O feature during deposition. Secondly, there is likely a direct reaction of the precursors with oxygen, similar to the self-cleaning effect reported for ALD on compound semiconductors.³⁷ Thus, the O-SMoS also acts as a sacrificial nucleation layer that, after reacting with the metal precursor, leaves a MoS₂ surface with S-O bonding below detectable limits. It is also noted that there is no detection of Mo-Al or S-Al chemical bonds, suggesting a non-covalent bonding of Al₂O₃ on MoS₂, similar to the case of HfO₂ on MoS₂.^{9,10}

In summary, a UV-O₃ treatment is an effective route to functionalizing the MoS₂ surface, and the presence of UV light was indispensable for S-O bond formation under the conditions employed here. DFT suggests two favorable oxygen adsorption sites (i.e., on top of sulfur or adsorption on sulfur vacancies), although the experimental evidence suggests that adsorption on sulfur is dominant, likely due to the low areal density of initial sulfur vacancy sites. In addition, the oxygen terminated MoS₂ surface was found to be ideal for ALD since Al₂O₃ thin films can be deposited uniformly on clean MoS₂, allowing precise control of dielectric thickness. These results demonstrate that UV-O₃ treatment is a practical and non-disruptive route for functionalization of MoS₂ while preserving its structural and electronic properties.

This work was supported in part by the Center for Low Energy Systems Technology (LEAST), one of six centers supported by the STARnet phase of the Focus Center Research Program (FCRP), a Semiconductor Research Corporation (SRC) program sponsored by MARCO and DARPA. It is also supported by the SWAN Center, a SRC center sponsored by the Nanoelectronics Research Initiative and NIST. The authors acknowledge Dr. Lanxia Cheng for useful discussions on remotely generated ozone reactions on MoS₂.

¹H. Iwai, *Microelectron. Eng.* **86**, 1520 (2009).

²Q. H. Wang, K. Kalantar-Zadeh, A. Kis, J. N. Coleman, and M. S. Strano, *Nat. Nanotechnol.* **7**, 699 (2012).

³W. Bao, X. Cai, D. Kim, K. Sridhara, and M. S. Fuhrer, *Appl. Phys. Lett.* **102**, 042104 (2013).

⁴B. Radisavljevic, A. Radenovic, J. Brivio, V. Giacometti, and A. Kis, *Nat. Nanotechnol.* **6**, 147 (2011).

- ⁵S. Kim, A. Konar, W.-S. Hwang, J. H. Lee, J. Lee, J. Yang, C. Jung, H. Kim, J.-B. Yoo, J.-Y. Choi *et al.*, *Nat. Commun.* **3**, 1011 (2012).
- ⁶H. Liu and P. D. Ye, *IEEE Electron Device Lett.* **33**, 546 (2012).
- ⁷S. Das, H.-Y. Chen, A. V. Penumatcha, and J. Appenzeller, *Nano Lett.* **13**, 100 (2013).
- ⁸S.-W. Min, H. S. Lee, H. J. Choi, M. K. Park, T. Nam, H. Kim, S. Ryu, and S. Im, *Nanoscale* **5**, 548 (2013).
- ⁹D. Jena and A. Konar, *Phys. Rev. Lett.* **98**, 136805 (2007).
- ¹⁰S. McDonnell, B. Brennan, A. Azcatl, N. Lu, H. Dong, C. Buie, J. Kim, C. L. Hinkle, M. J. Kim, and R. M. Wallace, *ACS Nano* **7**, 10354 (2013).
- ¹¹H. Liu, K. Xu, X. Zhang, and P. D. Ye, *Appl. Phys. Lett.* **100**, 152115 (2012).
- ¹²J. Yang, S. Kim, W. Choi, S. H. Park, Y. Jung, M.-H. Cho, and H. Kim, *ACS Appl. Mater. Interfaces* **5**, 4739 (2013).
- ¹³A. Pirkle, J. Chan, A. Venugopal, D. Hinojos, C. W. Magnuson, S. McDonnell, L. Colombo, E. M. Vogel, R. S. Ruoff, and R. M. Wallace, *Appl. Phys. Lett.* **99**, 122108 (2011).
- ¹⁴J. Chan, A. Venugopal, A. Pirkle, S. McDonnell, D. Hinojos, C. Magnuson, R. S. Ruoff, L. Colombo, R. M. Wallace, and E. M. Vogel, *ACS Nano* **6**, 3224 (2012).
- ¹⁵S. McDonnell, A. Pirkle, J. Kim, L. Colombo, and R. M. Wallace, *J. Appl. Phys.* **112**, 104110 (2012).
- ¹⁶L. Colombo, R. M. Wallace, and R. S. Ruoff, *Proc. IEEE* **101**, 1536 (2013).
- ¹⁷J. R. Williams, L. DiCarlo, and C. M. Marcus, *Science* **317**, 638 (2007).
- ¹⁸B. Lee, G. Mordì, M. J. Kim, Y. J. Chabal, E. M. Vogel, R. M. Wallace, K. J. Cho, L. Colombo, and J. Kim, *Appl. Phys. Lett.* **97**, 043107 (2010).
- ¹⁹M. J. Hollander, M. LaBella, Z. R. Hughes, M. Zhu, K. A. Trumbull, R. Cavaleiro, D. W. Snyder, X. Wang, E. Hwang, S. Datta *et al.*, *Nano Lett.* **11**, 3601 (2011).
- ²⁰C.-W. Chu, S.-H. Li, C.-W. Chen, V. Shrotriya, and Y. Yang, *Appl. Phys. Lett.* **87**, 193508 (2005).
- ²¹K. F. Mak, C. Lee, J. Hone, J. Shan, and T. F. Heinz, *Phys. Rev. Lett.* **105**, 136805 (2010).
- ²²R. M. Wallace, *ECS Trans.* **16**, 255 (2008).
- ²³See supplementary material at <http://dx.doi.org/10.1063/1.4869149> for the experimental and calculation details and a brief discussion on XPS intensity ratios, O₃ exposure without UV, surface morphology, and ALD uniformity.
- ²⁴N. M. D. Brown, N. Cui, and A. McKinley, *Appl. Surf. Sci.* **134**, 11 (1998).
- ²⁵J. R. Vig and J. W. Le Bus, *IEEE Trans. Parts, Hybrids, Packag.* **12**(4), 365 (1976).
- ²⁶J. R. Vig, *J. Vac. Sci. Technol. A* **3**, 1027 (1985).
- ²⁷Z. H. Lu, *J. Vac. Sci. Technol. B* **11**, 2033 (1993).
- ²⁸S. Zhao, S. P. Surwade, Z. Li, and H. Liu, *Nanotechnology* **23**, 355703 (2012).
- ²⁹A. Pirkle, Y. J. Chabal, L. Colombo, and R. M. Wallace, *Electrochem. Soc. Trans.* **19**(5), 215 (2009).
- ³⁰See Ref. 26, and references therein.
- ³¹B. L. Abrams and J. P. Wilcoxon, *Crit. Rev. Solid State Mater. Sci.* **30**, 153 (2005).
- ³²T. R. Thurston and J. P. Wilcoxon, *J. Phys. Chem. B* **103**, 11 (1999).
- ³³S. McDonnell, R. Addou, C. Buie, R. M. Wallace, and C. L. Hinkle, "Defect-Dominated Doping and Contact Resistance in MoS₂," *ACS Nano* (published online).
- ³⁴N. Karl and C. Guenther, *Cryst. Res. Technol.* **34**, 243 (1999).
- ³⁵C. Günther, N. Karl, and J. Pflaum, *Langmuir* **21**, 656 (2005).
- ³⁶H. S. Lee, S. Min, Y. Chang, M. K. Park, T. Nam, H. Kim, J. H. Kim, S. Ryu, and S. Im, *Nano Lett.* **12**, 3695 (2012).
- ³⁷C. L. Hinkle, A. M. Sonnet, E. M. Vogel, S. McDonnell, G. J. Hughes, M. Milojevic, B. Lee, F. S. Aguirre-Tostado, K. J. Choi, H. C. Kim, J. Kim, and R. M. Wallace, *Appl. Phys. Lett.* **92**, 071901 (2008).